EASR

Engineering and Applied Science Research

https://www.tci-thaijo.org/index.php/easr/index

Published by the Faculty of Engineering, Khon Kaen University, Thailand

Application of the HEC-HMS model for analysing land use change and hydrological responses across different return periods in tropical flood-prone areas

Suzani Mohamad*[1)], Zulfa Hanan Ashaari[1)], Mohammad Firuz Ramli[1)] and Balqis Mohamed Rehan[2)]

[1)]Department of Environment, Faculty of Forestry and Environment, Universiti Putra Malaysia, Serdang, Selangor, Malaysia
[2)]Department of Civil Engineering, Faculty of Engineering, Universiti Putra Malaysia, Serdang, Selangor, Malaysia

Received 28 March 2025
Revised 3 June 2025
Accepted 5 August 2025

Abstract

Land use change is a significant environmental concern worldwide today, as it has the potential to increase the frequency of natural disasters, such as floods. The Sg. Segamat Watershed, which is particularly vulnerable to flooding, highlights the importance of hydrological modelling as a crucial tool in disaster mitigation. In this study, the Hydrologic Engineering Center's Hydrologic Modelling System (HEC-HMS) was utilised to assess the effects of land use change on hydrological responses across various return periods. The analysis examined both the pre- and post-calibration phases under varying land use conditions. Land use data from 2006 and 2011 were used to simulate future scenarios. The findings showed that the expansion of built-up areas and the conversion of forested land to mixed agriculture had a significant influence on flood patterns. Specifically, built-up areas expanded by 2.24%, resulting in increased flood volumes in sub-basins 4, 9, and 12 between 2006 and 2026. Concurrently, forest cover declined by approximately 4.40%, which led to heightened flood peak heights in sub-basins 1, 3, and 11 under all land use conditions. Sub-basin 3 recorded the highest flood peak height, estimated at 1,150.20 m^3/s in the pre-calibration phase, 1,165.80 m^3/s in the post-calibration, and 1,036.20 m^3/s using the initial CN with calibrated parameters. Meanwhile, sub-basin 4 demonstrated the highest flood volume, with estimates reaching 342.10 mm pre-calibration, 366.09 mm post-calibration, and 341.04 mm using initial CN with calibrated parameters. These results clearly demonstrate how land use changes influence hydrological behaviour, emphasising the need for watershed planning and flood risk management. The study highlights the value of hydrological modelling as a tool for enhancing flood mitigation strategies and provides crucial insights for policymakers, planners, government agencies, and local communities.

Keywords: Land use change, HEC-HMS model, Hydrological modelling, Flood risk management, Flood peak heights, Flood volumes

1. Introduction

Humans now live in an environment sensitive to unexpected and extreme disasters. According to Makwana [1], disasters are a reality that cannot be inevitable in life, therefore, it is an alarming global concern. Floods are the most disastrous and recurrent natural disasters, destroying both property and human lives [2]. The word "flood" comes from the old English word "flod," which resembles the German word "flut," and the Dutch word "vloed," which expresses the inflow and float of water [3]. The world has witnessed many incidents of floods, and according to CRED [4], there were 201 events in 2020. Moreover, there seems to have been an increase in flood events, with 3254 from 2000 to 2019, as opposed to 1389 from 1980 to 1999 [5]. Between 1990 and 2016, global flood losses are estimated to have totalled USD 723 billion [6]. Floods may become more intense and frequent, indicating that in some places, the length and severity of floods have increased [7, 8]. Notably, floods were felt heavily across Africa and Asia [4].

Most of Malaysia's states are vulnerable to floods, such as Pahang, Kelantan, Johor, Perak, Kuala Lumpur, Selangor, Sabah and Sarawak. Historically, many Malaysians opted to live along the banks and floodplains of the main river, making watersheds highly attractive for urban development due to lowland areas [9, 10]. Therefore, this stimulates the severity of natural disasters when they occur [11]. Floods in Malaysia are worrisome because over 9% of the total land area, or over 29, 000 km^2, is flood-prone, potentially affecting over 4.82 million people and causing RM 915 million in damages [12]. According to Zawiah et al. [13], a massive flood in December 2006 and January 2007 in Johor is believed to be the costliest disaster in Malaysian history, resulting in a total loss of RM1.5 billion, the evacuation of 110,000 people, and 18 deaths. Rosmadi et al. [14] state that the frequency and magnitude of floods may worsen in the future due to land use changes that raise runoff rates, and climate change that causes more frequent heavy rainstorms, as well as the rise in sea level.

Correspondingly, Mohamad et al. [15] pointed out that land use changes could potentially impact flood risk. Thus, comprehension of land use change is critical when it comes to several planning and management activities, particularly when it comes to proposing solutions to social, economic, and environmental problems. Furthermore, investigation of land use and its changes is particularly important, especially in watersheds, as they play a key role in altering hydrological processes. These changes impact runoff characteristics and related factors such as evaporation, transpiration, streamflow, and groundwater recharge, because land use and hydrology are intertwined and are seen as affecting watershed hydrology [16, 17]. Additionally, the expansion of urban areas, as an

*Corresponding author.
Email address: suzanimohamad@gmail.com
doi: 10.14456/easr.2025.54

example, increases impervious surfaces while decreasing pervious surfaces, reducing infiltration capacity, interfering with evapotranspiration, increasing stormwater runoff, reducing the peak time of flood hydrographs as well as driving up the risk of flooding [18, 19].

Hydrological simulation models are valuable for designing effective flood mitigation strategies to address flood risks that are posed by land use change. The Hydrologic Modelling System (HEC-HMS), developed by the US Army Corps of Engineers' Hydrologic Engineering Centre (HEC), is a popular hydrological modelling instrument. HEC-HMS is used worldwide thanks to its free online accessibility, user-friendly design, minimal input data requirements, trustworthy findings, capacity to simulate both short- and long-term events, numerous method options, and accurate prediction of spatiotemporal catchment responses. It is additionally compatible with small unmeasured watersheds and complex watershed simulations [20-22]. Many research efforts used the HEC-HMS to investigate the impact of land use changes on hydrological responses. Notably, Al-Samawi et al. [23] as well as Setiawan and Nandini [24] have discovered that converting agricultural land to built-up areas significantly leads to changes in runoff characteristics, resulting to disruptions in the natural water balance. According to Ata et al. [25], hydrological parameters are determined by curve number analysis. The decrease of open spaces and water bodies caused by urban expansion contributes to a higher proportion of impervious land and CN values, which in turn alter the hydrological regime and increase the potential risk of flooding. Furthermore, deforestation and expanding agriculture also led to increased surface runoff [26, 27]. Land use changes significantly affect flood volume, peak discharge, and flood area. Farid et al. [28] posit that converting 13 km² of forest or agricultural land to urban areas or bare soil increases flood area, flood peak height, and flood volumes by 15%, 3.6%, and 16%, respectively. Hence, this study aims to assess the applicability of the HEC-HMS model for analysing the effect of land use change on hydrological responses in the Sg. Segamat Watershed, Malaysia. It also attempts to investigate the effect of land use change on flood peak heights and flood volumes across different return periods, considering i) pre-calibration, and ii) post-calibration under varying land use conditions. The initiative sought to offer a comprehensive knowledge of the potential impact of land use change on watershed hydrology, with a sense of the intention of enhancing knowledge of hydrological processes and designing effective flood mitigation strategies.

2. Materials and methods

2.1 Study area description

The Sg. Segamat watershed is located in the Segamat district of southern Peninsular Malaysia, positioned between latitudes 2° 25′ N and 2° 42′ N, and longitudes 102° 45′ E and 103° 10′ E. The watershed covers an area of approximately 694.58 km², with the Segamat River serving as the main river (Figure 1). The watershed spans around 61.8 kilometres and ranges in width from 9 to 90 meters. The annual rainfall ranges from 1,400 to 2,000 mm; notwithstanding, the average monthly flow has a potential of 191 m³/s during a large flood [29].

This watershed was prone to flooding and regularly experiences both small and major floods during periods of heavy rainfall. As a tropical river system, this watershed was at risk of two flood peaks: one triggered by monsoon-induced rainfall and another by equatorial convective rainfall [30]. Flooding occurs regularly in December, considering this area experiences the highest rainfall and peak streamflow [31, 32]. Furthermore, Segamat town is situated within this watershed, and since the 1950s, this town has faced several major floods. The 2011 flood was estimated to have caused damages of up to USD 146.2 million [29].

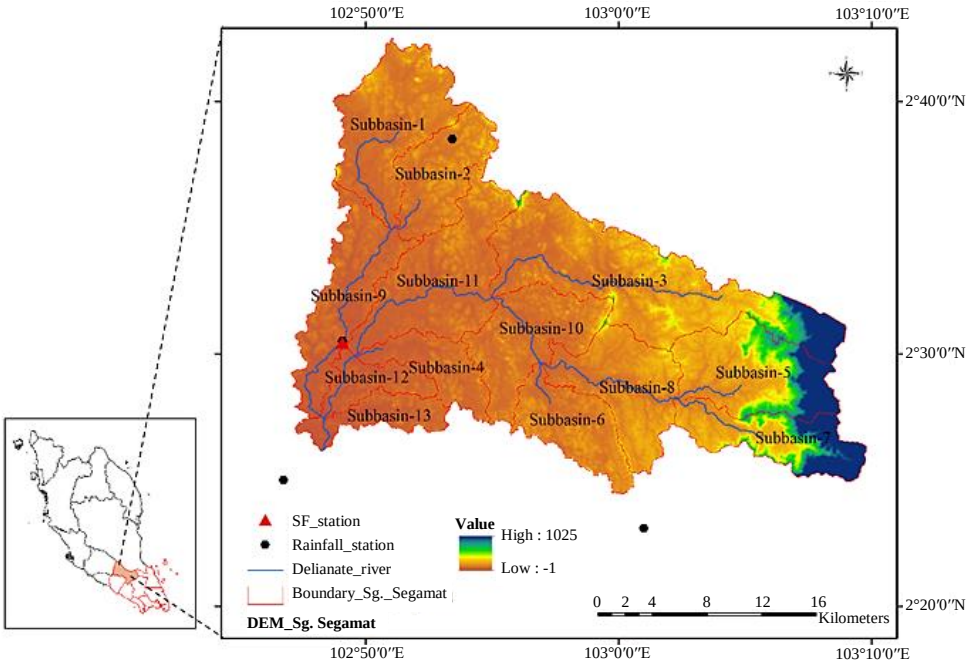

Figure 1 The Sg. Segamat watershed's geographical location in the Segamat district

2.2 Data sources

The input data for the HEC-HMS model consists of land use maps, digital elevation model (DEM), soil properties, as well as daily rainfall and flow discharge data. In this study, (i) land use data for 2006 and 2011 were derived from 30m resolution Landsat images accessed via https://earthexplorer.usgs.gov, while land use data for 2016 were obtained from SPOT imagery provided by the Agency

of Remote Sensing Malaysia (ARSM); (ii) the Shuttle Radar Topography Mission (SRTM) DEM with 30m resolution was sourced from the USGS Earth Explorer website (https://earthexplorer.usgs.gov); (iii) soil property data was acquired from Malaysia's Department of Agriculture; and (iv) daily rainfall and flow discharge data were obtained from Malaysia's Department of Irrigation and Drainage (DID). The daily rainfall and flow discharge datasets span the period from 1971 to 2020. In this study, the annual maximum rainfall values were used to calculate various return periods using the Generalised Extreme Value (GEV) distribution. The estimated rainfall for different return periods in the Sg. Segamat watershed is presented in Table 1.

Table 1 The estimated rainfall for return periods in the Sg. Segamat watershed

Return period, T (years)	Rainfall (mm)
2	68.70
5	100.21
10	129.46
25	179.85
50	230.19
100	294.63
200	377.32

2.3 Modelling the Impact of land use change on hydrological responses

Figure 2 depicts the general framework for investigating the impact of land use change on flood peak heights and flood volumes using the HEC-HMS model. The study was designated into two phases: 1) assessing the spatial-temporal land use, and 2) hydrological modelling to estimate flood peak heights and flood volumes.

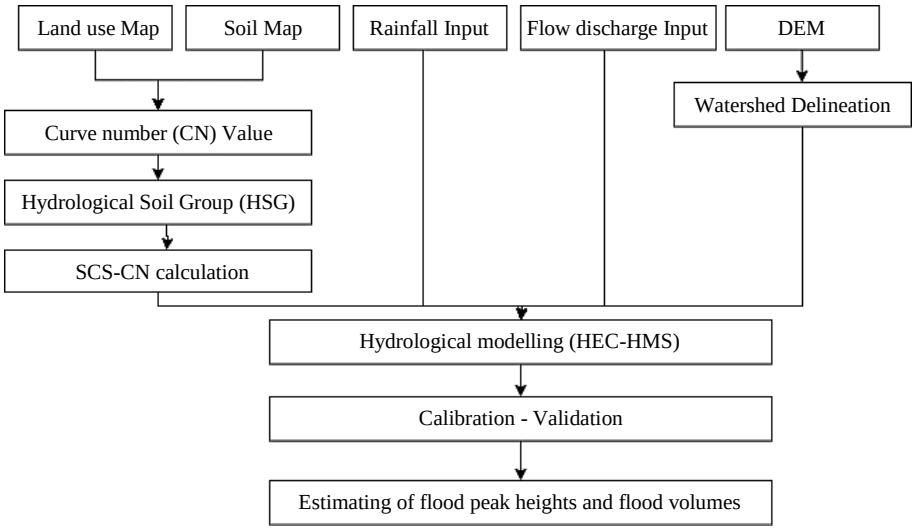

Figure 2 The flowchart of methodology for investigating the impact of land use change on flood peak heights and flood volumes

2.3.1 Assessing the spatial-temporal land use

In the first phase, the spatial-temporal land use was assessed. The proportion of land use in the Sg. Segamat watershed was extracted from the land use data for the Segamat district. In the pre-processing stage, satellite imagery underwent geometric correction, mosaicking, and sub-setting using ArcGIS 10.4. Subsequently, unsupervised (ISODATA) and supervised (Maximum Likelihood Classification, MLC) classification methods were applied using ENVI 5.1. The accuracy of the generated land use maps was evaluated using Equations (1–4), and the overall classification accuracy is presented in Table 2.

$$OA = \frac{\sum_{i=1}^{r} n_{ii}}{N} \quad (1)$$

$$PA_i = \frac{n_{ii}}{n_{+i}} \quad (2)$$

$$UA_i = \frac{n_{ii}}{n_{i+}} \quad (3)$$

$$KC = \frac{N\sum_{i=1}^{r} n_{ii} - \sum_{i=1}^{r}(n_{i+}n_{+i})}{N^2 - \sum_{i=1}^{r}(n_{i+}n_{+i})} \quad (4)$$

Where, N signifies the total number of pixels, n_{ii} represents the count of correctly classified pixels, n_{i+} is the number of pixels in the land use map, n_{+i} corresponds to the number of pixels in the land use map, r stands for the total number of classes, and i denotes the particular i^{th} class.

Table 2 Classification accuracy assessments of the Segamat district from 2006 to 2016 using the error matrix

Land use	Landsat				SPOT	
Class	2006		2011		2016	
	UA	PA	UA	PA	UA	PA
Built-up areas	90	90	85	94.44	70	100
Forest	100	76.92	100	90.91	100	86.96
Mixed agriculture	87.50	85.37	92.50	82.22	97.50	78
Water bodies	65	100	75	100	65	100
OA	86 %		89 %		86 %	
KC	0.81		0.85		0.80	

Note: The abbreviations UA, PA, OA, and KC represent user's accuracy, producer's accuracy, overall accuracy and Kappa coefficient, respectively. (Source: Mohamad et al. [15])

The CA-Markov model was utilised to forecast land use in 2016, 2021, and 2026, using ArcGIS 10.4 and IDRISI Selva 17.0. Factors such as slope, distance from residential areas, roads, and water bodies were considered in developing the criteria for Multi-Criteria Evaluation (MCE). The equations for the Markov Chain (MC) and Cellular Automata (CA) models are provided in Equations 5–7.

$$P_{ij} = \begin{bmatrix} P_{11} & \cdots & P_{1n} \\ \vdots & \vdots & \vdots \\ P_{n1} & \cdots & P_{nn} \end{bmatrix} \tag{5}$$

$$0 \leq P_{ij} < 1 \; and \sum_{j=1}^{n} P_{ij} = 1, i, j = 1, 2, \cdots, n \tag{6}$$

$$S_{t+1} = P_{ij} \times S_t \tag{7}$$

Where, S represents the land use status, n is the number of land use categories, P_ij is the probability matrix for state transitions, and t; t+1 are the respective time points.

$$S_{t+1} = f(S_t, N) \tag{8}$$

For the finite cells, S stands for the set of states, t and t+1 refer to distinct time moments, N represents the cell neighbourhood, and f is the local spatial transformation rule. Land use forecasting for the years 2021 and 2026 was undertaken after the model validation, which compared the actual 2016 data with simulated land use data. The model's performance, with a kappa statistic over 0.8, demonstrates that the model is reliable in forecasting future land use patterns. Figure 3 presents the flowchart of the methodology for assessing spatial-temporal land use, with a detailed explanation of the technique outlined in Mohamad et al. [15].

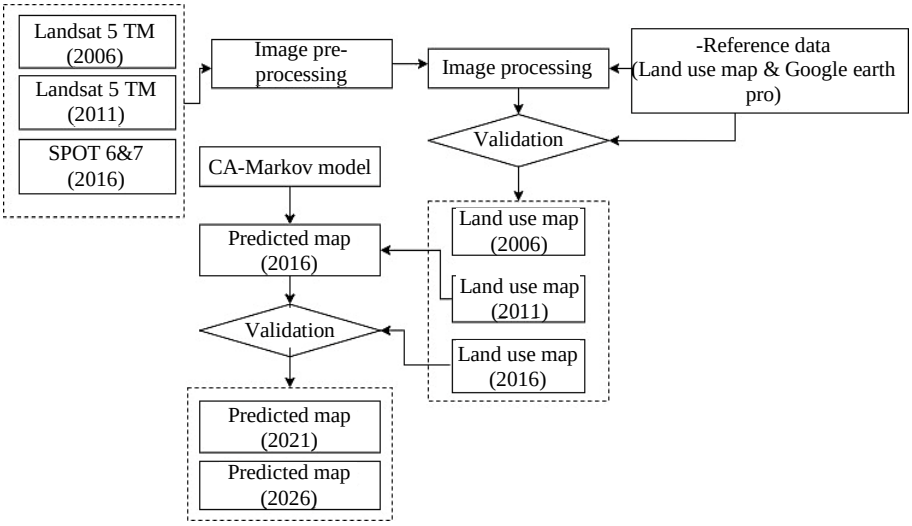

Figure 3 The flowchart of methodology for assessing spatial-temporal land use

2.3.2 Hydrological modelling to estimate flood peak heights and flood volumes

The watershed's hydrological response to land use changes was subsequently simulated to estimate flood peak heights and flood volumes. The watershed was delineated using the DEM in the HEC-HMS model. Watershed loss rates were calculated using the Soil Conservation Service–Curve Number (SCS–CN) technique, as shown in Equations 9 and 10. The CN value was calculated by integrating the land use and soil data.

$$Q = \frac{(P - 0.2S)^2}{P + 0.8S} \quad (9)$$

$$S = \frac{25400}{CN} - 254 \quad (10)$$

In this situation, Q signifies direct runoff (mm), P indicates rainfall (mm), Ia represents initial abstraction (ordinarily about 0.2S), S is for possible maximum soil retention (mm), and CN is the curve number. Direct runoff was calculated using the Soil Conservation Service Unit Hydrograph (SCS UH) model, as seen in Equations 11 to 13.

$$T_c = \frac{L^{0.8}\ (S + 1)^{0.7}}{1140 Y^{0.5}} \quad (11)$$

$$T_L = 0.6\ T_c \quad (12)$$

$$S = \frac{1000}{CN} - 10 \quad (13)$$

The lag time (h), concentration time (h), flow length (ft), average watershed land slope (%), and maximum potential retention are denoted as TL, TC, L, Y, and S, respectively.

2.3.3 Accuracy evaluation methods

The model calibration in this study was conducted from December 3 to December 31, 2007, with the validation period running from December 4 to December 31, 2019. The Nash-Sutcliffe efficiency (NSE) and per cent t bias (PBIAS) were used to assess the performance of the HEC-HMS model, as detailed in Equations 14 and 15.

$$NSE = 1 - \frac{\sum_{i=1}^{n}(Q_i - P_i)^2}{\sum_{i=1}^{n}(Q_i - \bar{Q})^2} \quad (14)$$

$$PBIAS = \frac{\sum_{i=1}^{n}(Q_i - P_i)(100)}{\sum_{i=1}^{n} Q_i} \quad (15)$$

Specifically, Q_i indicates the observed flow, P_i is the simulated flow, n represents the number of observed or simulated data points, and $\bar{Q}$ is the observed flow mean, all are expressed in m³/s. As indicated in Table 3, the model with the initial parameters (pre-calibration) shows low reliability; however, after calibration (post-calibration), the results achieve satisfactory outcomes, aligning with the findings of Eryani et al. [33]. This improvement can be attributed to the use of both manual and automated calibration methods, which enabled a close agreement between simulated and observed values. The same approach was utilised by Skhakhfa and Ouerdachi [34] and Carlos Mendoza et al. [35].

Table 3 Performance evaluation of the hydrological model during calibration and validation

	Pre-calibration		**Post-calibration**	
	NSE	**PBIAS**	**NSE**	**PBIAS**
		Land use 2006		
Calibration	0.351	-53.08%	0.504	-49.64%
Validation	0.357	-14.62%	0.563	-3.14%
		Land use 2011		
Calibration	0.354	-52.99%	0.507	-48.79%
Validation	0.353	-14.31%	0.581	-0.03%
		Land use 2016		
Calibration	0.355	-52.78%	0.520	-48.44%
Validation	0.336	-13.64%	0.504	1.19%
		Land use 2021		
Calibration	0.355	-52.61%	0.516	-48.30%
Validation	0.319	-13.04%	0.527	1.73%
		Land use 2026		
Calibration	0.355	-52.56%	0.505	-48.14%
Validation	0.314	-12.86%	0.534	2.35%

The HEC-HMS model parameters, including Curve Number (CN), Initial Abstraction (Ia), percentage of impervious area, and time lag (TL), were calculated to estimate flood peak heights and flood volumes under various land use conditions. Additionally, standard error (SE) was used to evaluate the accuracy of the HEC-HMS model parameters pre- and post-calibration, with smaller SE values indicating more reliable and consistent model performance [36]. The outcomes of both pre- and post-calibration for selected sub-basins in the Sg. Segamat watershed are provided in Tables 4 and 5, meanwhile, Table 6 indicates the sub-basins with the most and least significant flood responses.

Table 4 The estimation of impervious (%) and Curve Number (CN) for HEC-HMS model parameters

Sub-basin	Pre- calibration				Post- calibration	
	Impervious (%)		Curve Number (CN)			
	2006	2026	2006	2026	2006	2026
Subbasin-1	0.03	0.01	82.84	83.00	93.31	96.71
Subbasin-3	0.39	0.54	73.26	75.32	82.52	87.76
Subbasin-4	23.40	32.88	83.25	83.99	93.77	97.87
Subbasin-9	10.52	16.95	84.42	84.55	95.09	98.52
Subbasin-11	6.09	8.36	83.21	83.50	93.73	97.29
Subbasin-12	20.43	29.88	83.45	83.82	94.00	97.67
Standard Error (SE)			1.71	1.42	1.93	1.66

Table 5 The estimation of Initial abstraction (Ia) and Lag Time for HEC-HMS model parameters

Sub-basin	Pre- calibration		Post- calibration		Pre- calibration		Post- calibration	
	Initial abstraction (Ia)				Lag Time			
	2006	2026	2006	2026	2006	2026	2006	2026
Subbasin-1	10.53	10.40	12.09	12.12	188.40	187.39	218.78	218.34
Subbasin-3	18.54	16.64	21.30	19.39	282.72	266.62	328.29	310.66
Subbasin-4	10.22	9.69	11.74	11.29	160.20	156.26	186.03	182.07
Subbasin-9	9.38	9.28	10.77	10.82	229.37	228.31	266.35	266.03
Subbasin-11	10.25	10.04	11.77	11.70	226.79	224.65	263.35	261.77
Subbasin-12	10.08	9.81	11.57	11.43	175.49	173.31	203.78	201.94
Standard Error (SE)	1.42	1.14	1.63	1.33	18.33	16.74	21.29	19.51

Table 6 Flood peak heights and flood volumes estimation using pre-, post and initial CN value with calibrated parameters input by sub-basin in Sg. Segamat watershed

Subbasin	FPH		FV	
	2006	2026	2006	2026
Pre- calibration				
Subbasin-1	863.2	867.2	320.79	321.36
Subbasin-3	1083	1150.2	285.47	293.51
Subbasin-4	384.6	398.7	335.13	342.1
Subbasin-9	618.9	623.8	331.72	335.38
Subbasin-11	833.9	840.4	325.46	327.65
Subbasin-12	274.5	278.3	334.05	340.11
Post calibration				
Subbasin-1	823.9	839.1	347.89	356.76
Subbasin-3	1054.1	1165.8	309.54	325.97
Subbasin-4	378.4	386.5	355.97	366.09
Subbasin-9	596	603.8	356.35	365.2
Subbasin-11	811.4	828.3	351.02	360.24
Subbasin-12	265.4	270.5	355.76	365.13
Initial CN value with calibrated parameters				
Subbasin-1	761.6	764	319.26	319.67
Subbasin-3	961.6	1036.2	282.83	290.87
Subbasin-4	359.1	367.4	333.98	341.04
Subbasin-9	558.6	563	330.49	334.12
Subbasin-11	755.4	763.1	324.05	326.15
Subbasin-12	250.6	255.3	332.88	338.99

Note: the abbreviations FPH, and FV represent Flood peak heights and flood volumes, respectively.

3. Results and discussion

3.1 Land use change analysis

A significant proportion of land use in the Sg. Segamat watershed had been occupied by mixed agriculture, which covered more than 75% of the area (Figure 4). The forest was the dominant feature after mixed agriculture, which covered more than 18% in 2006, however, the percentage experienced a decrease in the subsequent years, namely in 2021 and 2026, reaching 14% of the area. Built-up areas and water bodies seem to be less dominant in the Sg. Segamat watershed. The built-up area covered about 3.66 - 5.90%, while water bodies covered less than 2%. During the 20 years of land use observation, increases in land use changes took place in built-up areas and a decrease in the percentage of forest.

Simultaneously, the spatial distribution of land use (Figure 5) indicates that the southwestern of the watershed has undergone the most significant urbanisation. This is primarily due to the presence of the district's main town within the watershed, which stimulates the development of built-up areas. Camara et al. [9] and Baig et al. [37] highlight that low-elevation watersheds are more vulnerable to urbanisation due to their greater exposure to anthropogenic pressures, in contrast to the mountainous and forested regions. The Sg. Segamat watershed, characterised by predominantly flat and low-lying terrain, allows 56.31% of the area to be considered suitable for development [38]. Furthermore, population growth strongly affects land use, with more housing demand causing expansion in built-

up areas [39]. The Segamat Local Plan 2030 Draft Report predicts the population will rise from 182,985 in 2010 to 215,029 by 2030 [38].

Malaysia emerged as one of the world's leading palm oil producers, which has driven the conversion of forest land in the Sg. Segamat watershed into oil palm plantations, contributing to forest fragmentation in Johor. Johor accounts for the largest share of the country's 5.74 million hectares of oil palm plantations, with Segamat district alone managing 90,590.63 hectares [38]. Rubber is the second most important crop in Segamat, occupying over 60,000 hectares, while nearly 13,000 hectares are used for growing fruits, vegetables, herbs, and spices. Recognising agriculture as a vital economic sector, the government aims to bolster Segamat's position as a major agricultural hub by introducing various initiatives, including enhanced investment incentives, infrastructure improvements to mitigate flood risks, better agricultural market data systems, and technical assistance for farmers. Shikur [40], agricultural policies focus on enhancing income and social well-being in rural areas through technological advancement, labour optimisation, research, and improved infrastructure. Despite the decrease in forest land, the establishment of Endau-Rompin National Park–as a Permanent Forest Reserve, has played a key role in forest conservation and supporting ecotourism by enhancing transportation and tourism facilities [38].

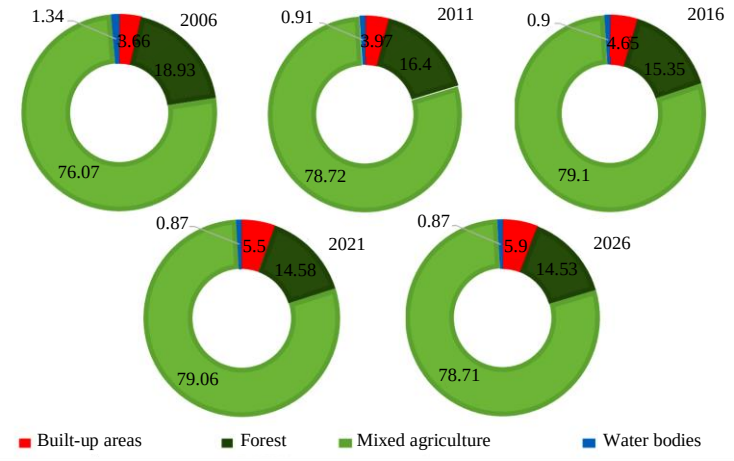

Figure 4 Percentage area of each class in Sg. Segamat watershed from 2006 to 2026

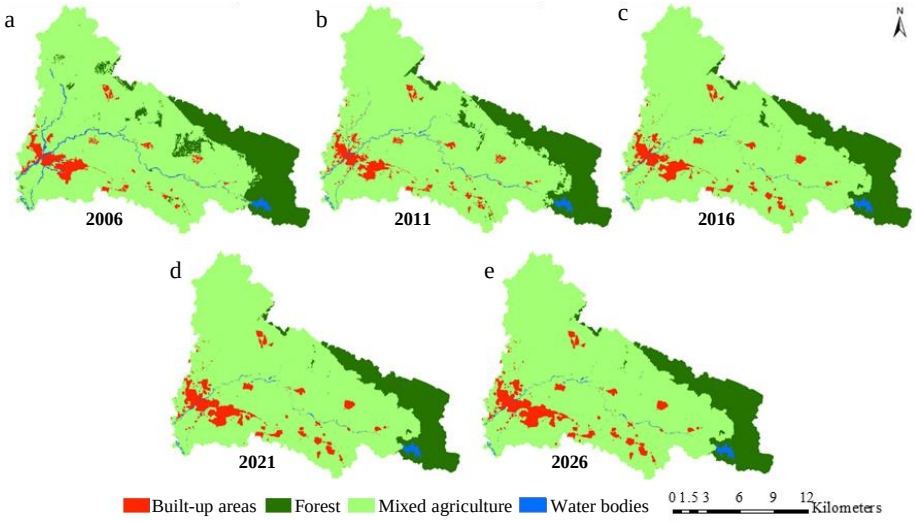

Figure 5 Spatial patterns of land use in Sg. Segamat watershed from 2006 to 2016: (a) 2006, (b) 2011, (c) 2016, (d) 2021 and (e) 2026

3.2 Impact of alterations in land use on estimates of flood peak heights and flood volumes across various return periods under varying land use conditions

The relationship between land use change and flood peak heights and flood volumes was investigated across return periods of 2 to 200 years in order to determine if varying land use conditions affected flood characteristics. The initial findings indicated that the flood peak heights across various return periods between the land use conditions, ranged from 178.20 to 2251.70 m³/s in 2006, 184.00 to 2300.40 m³/s in 2011, 190.00 to 2349.00 m³/s in 2016, 192.60 to 2360.90 m³/s in 2021, and from 193.4 to 2365.9 m³/s in 2026 (Figure 6a). Subsequently, the post-calibration (Figure 6b) flood peak heights varied between 210.50 to 2072.50 m³/s in 2006, 250.60 to 2223.70 m³/s in 2011, 310.40 to 2632.40 m³/s in 2016, 331.9 to 2796.30 m³/s in 2021, and 360.20 to 3054.30 m³/s in 2026.

Meanwhile, the flood volumes pre-calibration ranged from 26.88 to 308.58 mm in 2006, 27.17 to 309.25 mm in 2011, 27.78 to 310.69 mm in 2016, 28.39 to 231.69 mm in 2021, and 28.59 to 232.04 mm in 2026 (Figure 7a). Post calibration (Figure 7b), ranged from 32.93 to 287.63 mm land use conditions in 2006. Accordingly, there are 38.32 and 332.44 mm land use conditions in 2011, 40.50 and 342.14 mm land use conditions in 2016, 41.17 and 343.19 mm land use conditions in 2021, and 41.95 and 344.36 mm land use conditions in 2026.

The uncertainty analysis of HEC-HMS parameters indicated that the SE values were smaller in pre-calibration as opposed to post-calibration (Tables 4 and 5). Consequently, the study incorporates the initial CN value with calibrated lag time and Ia to better investigate their influence on flood characteristics, particularly due to the rise in CN post-calibration. According to Cotugno et al. [41], a higher CN value allows more precipitation to contribute to surface runoff and flow into the river as opposed to infiltrating the ground, leading to severe floods. Therefore, the initial CN value with calibrated input parameters ranged from 147.40 to 1914.90 m³/s in 2006, 159.10 to 2024.20 m³/s in 2011, 189.50 to 2393.10 m³/s in 2016, 199.9 to 2538.60 m³/s in 2021, and 213.90 to 2754.40 m³/s in 2026 for flood peak heights (Figure 6c). At the same time, flood volumes (Figure 7c) varied from 23.52 to 264.80 mm in 2006, 25.27 to 300.35 mm in 2011, 26.41 to 308.69 mm in 2016, 27.02 to 309.98 mm in 2021, and 27.19 to 310.26 mm in 2026. Notwithstanding the post-calibration uncertainties in the HEC-HMS parameters, the model results indicate that flood peaks for a 200-year return period exceed 2,000 m³/s, which is consistent with the estimate of 2,642.0 m³/s that is reported by Romali and Yusop [42] using the Generalised Pareto distribution.

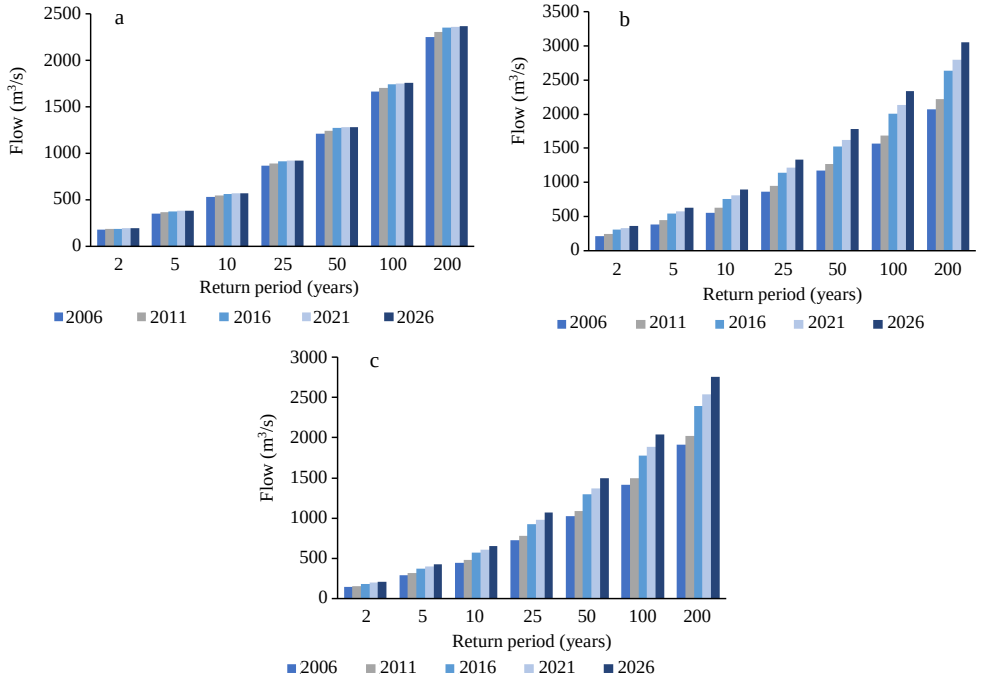

Figure 6 The estimation of flood peak heights: a) Pre-calibration, b) Post-calibration, c) Initial CN value with calibrated parameters input in Sg. Segamat watershed

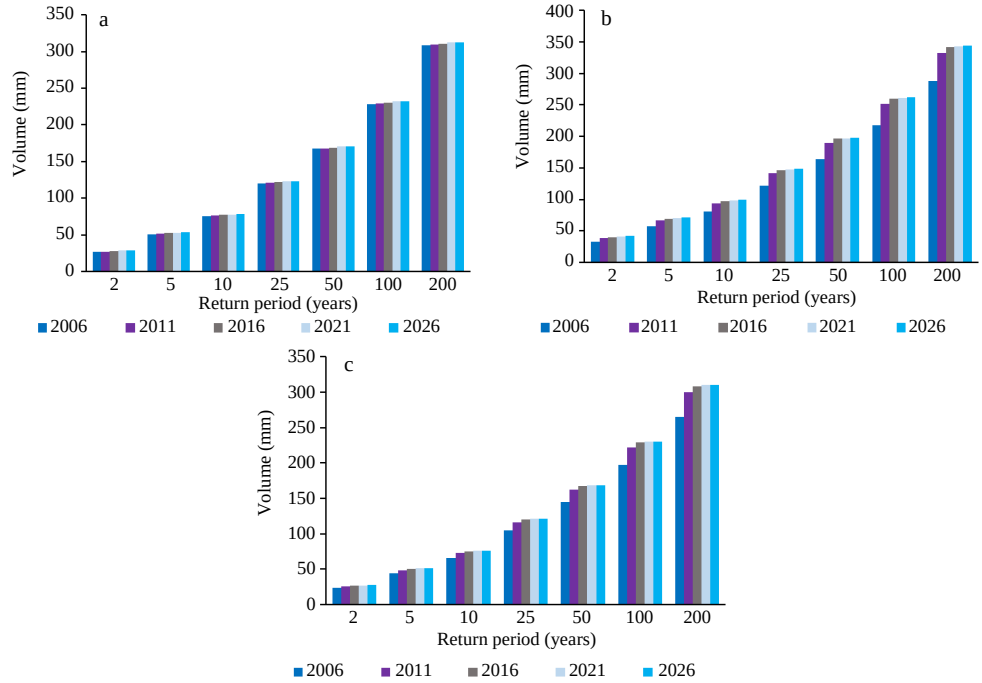

Figure 7 The estimation of flood volumes: a) Pre-calibration, b) Post-calibration c) Initial CN value with calibrated parameters input in Sg. Segamat watershed

3.3 Impact of alterations in land use on hydrological responses across sub-basins

Sub-basins 1, 3, and 11 in the Sg. Segamat Watershed recorded the highest flood peak heights (Figures 8, 9 and 10), while sub-basins 4, 9, and 12 recorded the highest flood volumes in all land use conditions (Figures 11, 12 and 13). Notably, sub-basin 3's significant flood peak heights was influenced by factors such as the percentage of impervious area, CN values, Ia, and lag time. Between 2006 and 2026, sub-basin 3's impervious area increased from 0.39% to 0.54%, CN values rose from 73.26 to 75.32, Ia decreased from 18.54 to 16.64, and lag time shortened from 282.72 minutes to 266.62 minutes during pre-calibration (Table 4-5). These changes resulted in flood peak heights ranging from 1,083 m³/s to 1,150.2 m³/s (Table 6). Despite mixed agriculture dominating sub-basins 1, 3, and 11, and forests being present in sub-basins 3 and 11, these sub-basins reveal higher flood peak heights, which may have been due to deforestation for the conversion of forest land to mixed agriculture. This is due between 2006 and 2026, the percentage of forests is expected to decrease by 4.4%, at the same time mixed agriculture is expected to expand by approximately 2.64%. Vegetation cover is widely recognised for mitigating flood peak heights through runoff delay. Fu et al. [43] as well as Setiawan and Nandini [24] have observed that woodland and grassland reduce unit flood peak heights more effectively than cropland. Therefore, declining forest cover results in higher flood peak heights.

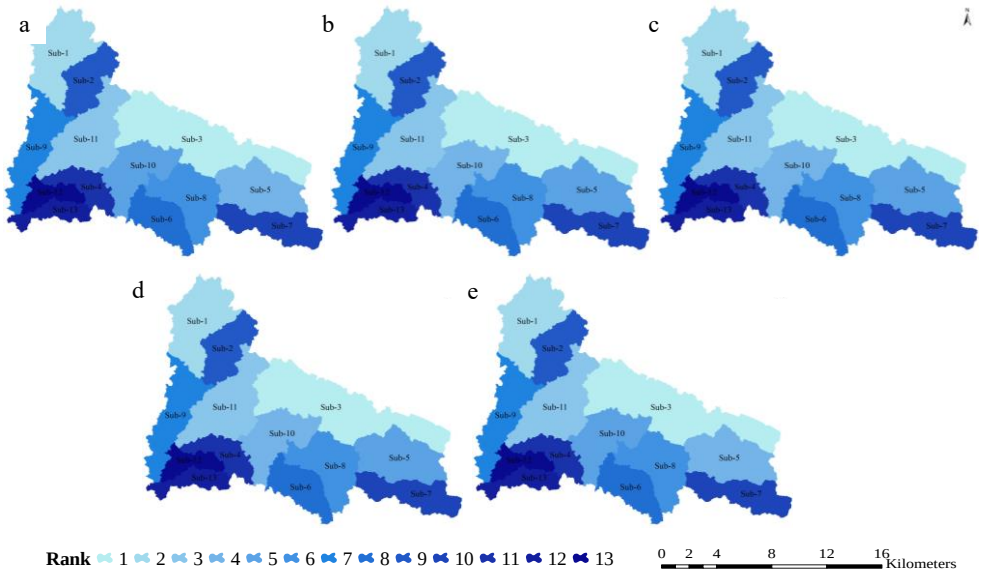

Figure 8 Rank of flood peak heights using Pre-calibration input for land use condition from 2006 to 2026: (a) 2006, (b) 2011, (c) 2016, (d) 2021, and (e) 2026

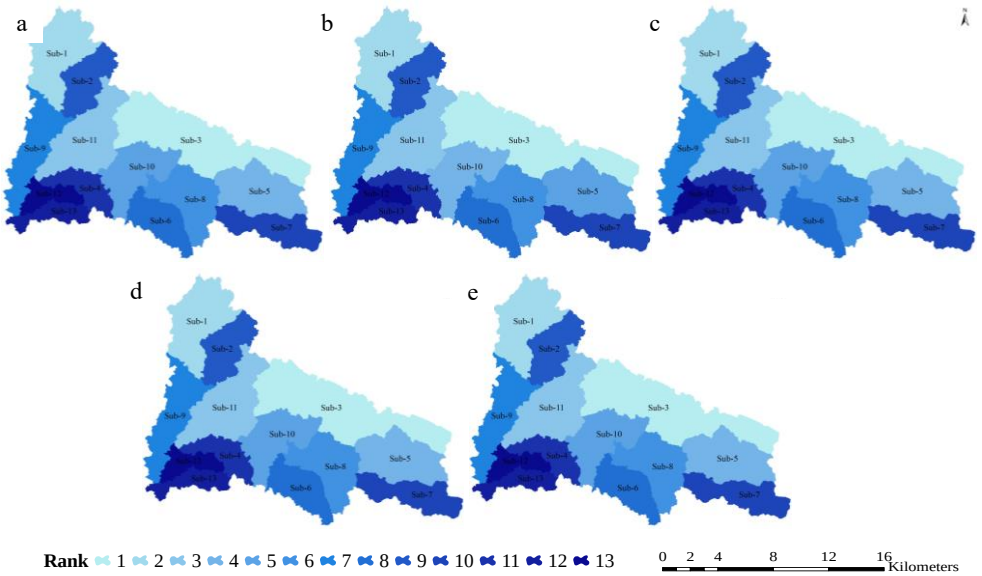

Figure 9 Rank of flood peak heights using Post-calibration parameters input for land use condition from 2006 to 2026: (a) 2006, (b) 2011, (c) 2016, (d) 2021, and (e) 2026

The expansion of impervious surfaces and development are probably the contributing factors in the increased flood volumes that are observed in sub-basins 4, 9, and 12, particularly as Segamat town is situated within these areas. For instance, sub-basin 4 recorded the highest percentage of impervious area from 2006 to 2026, increasing from approximately 23.40% to 32.88% (Table 4), partly because of the presence of Segamat Town. This led to CN values ranging from 83.25 to 83.99 and initial abstraction (Ia) values

declining from 10.22 to 9.69 during the pre-calibration period. Meanwhile, the lag time decreased from 160.20 minutes to 156.26 minutes, resulting in flood volumes of up to 335.13 mm and 342.1 mm for a 200-year return period (Table 5-6). Consequently, a decrease in recharging zones due to an increase in built-up area leads to an increase in run-off [44]. These findings underscore the importance of monitoring and managing the sub-basins in Table 6 due to their tendency to generate extreme flood peak heights and flood volumes, contributions that pose a serious hazard to downstream communities.

The HEC-HMS model effectively captured flood peak heights and flood volumes in the Sg. Segamat watershed, which aligned with similar studies. For instance, Abdulkareem et al. [45] demonstrated that deforestation of approximately 54.35% in 2013 significantly influenced flood peak heights, with a recorded value of 1,252.7 m³/s in Malaysia's Kelantan River basin. Similarly, Santillan et al. [46] observed increased flood peak heights from 888.87 to 1,167.81 million m³ at a 25-year return period due to deforestation from 67.7% to 62.8% and an increase in agricultural land from 12.2% to 15.5% between 1995 and 2017 in the Agusan River Basin, Philippines. Kuntiyawichai et al. [47] found that decreasing agricultural land by 1.7% and forested area by 19.5% were due to increases in residential area (51.5%) and industrial area (245.1%), which were expected to increase the average maximum daily outflow flood peak heights (baseline) from 1,051.6 to 1,273.6 m³/s for 25- and 100-year return periods. Farid et al. [28] reported that changing the land cover is expected to increase the flood area, flood peak heights, and flood volume. The flood area, flood peak heights, and volume of the flood are estimated to increase by 15%, 3.6%, and 16%, respectively, for every 13 km² of forest or agricultural land converted to bare soil or urban expansion in the Ciliwung River Basin, Indonesia. Between 1990 to 2020, dryland farming and settlement increased by about 59% and 161%, respectively. In addition, the decline was experienced by forests (19%) and shrubs (59%). Therefore, sub-basin W7 was the most affected, with flood peak heights increasing from 29.70 m³/s in 1990 to 41.58 m³/s in 2020 in Sari Watershed, Indonesia [24].

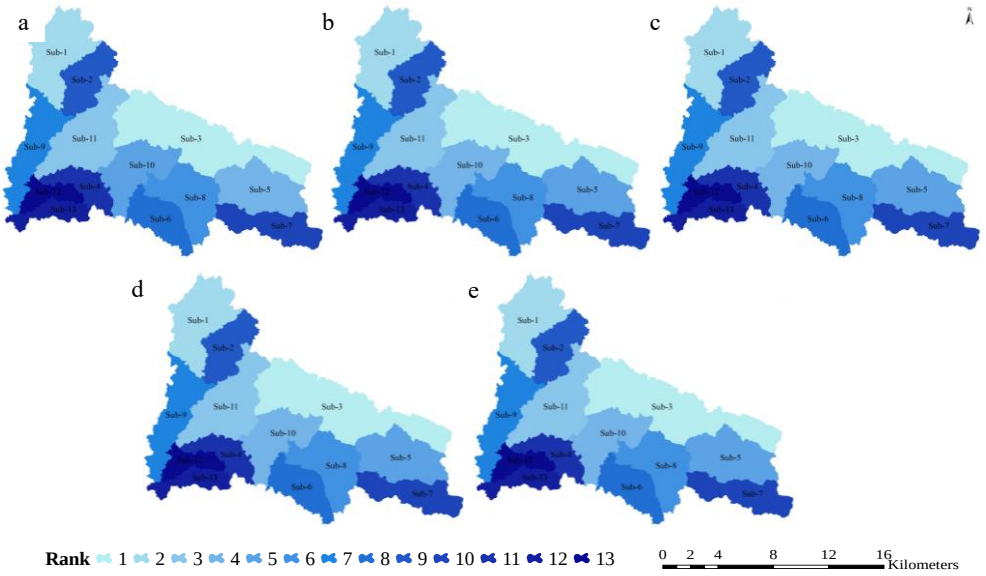

Figure 10 Rank of flood peak heights using the Initial CN value with calibrated parameters input for land use condition from 2006 to 2026: (a) 2006, (b) 2011, (c) 2016, (d) 2021, and (e) 2026

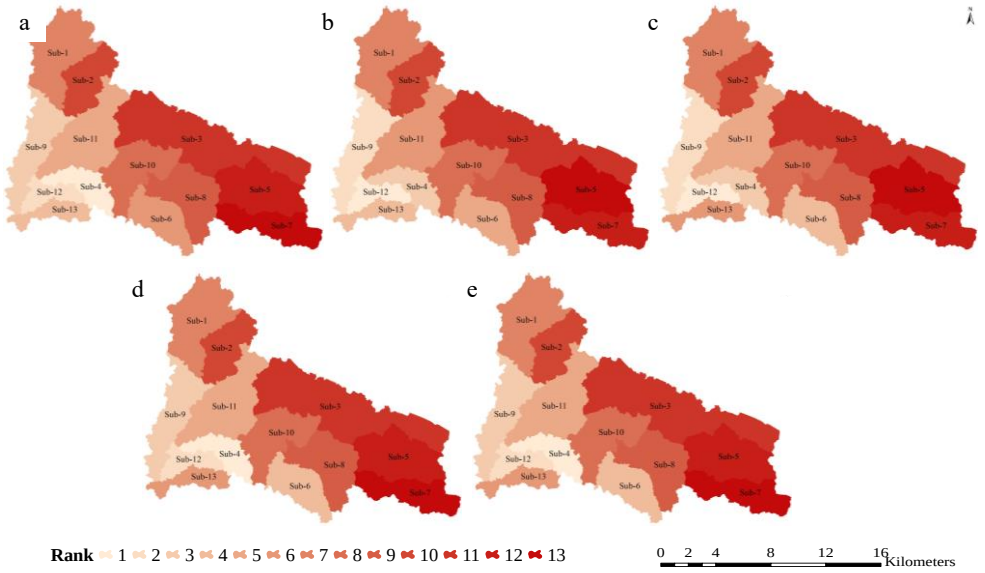

Figure 11 Rank of flood volumes using Pre-calibration input for land use condition from 2006 to 2026: (a) 2006, (b) 2011, (c) 2016, (d) 2021, and (e) 2026

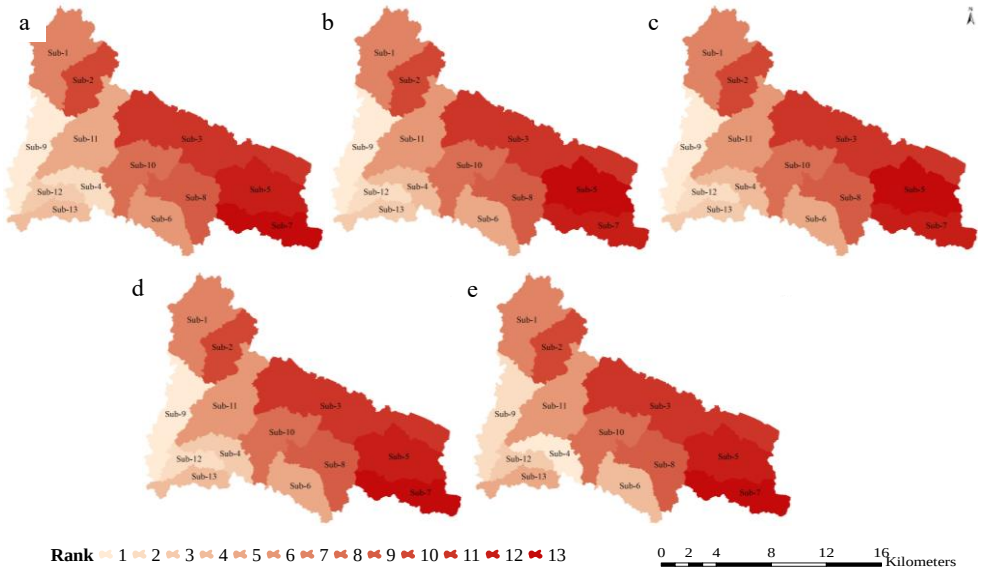

Figure 12 Rank of flood volumes using Post-calibration parameters input for land use condition from 2006 to 2026: (a) 2006, (b) 2011, (c) 2016, (d) 2021, and (e) 2026

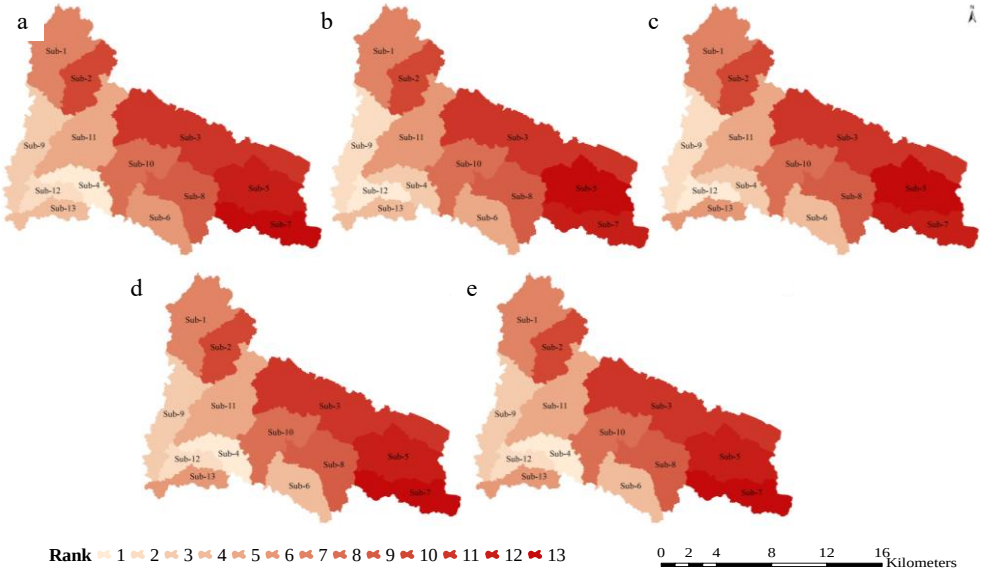

Figure 13 Rank of flood volumes using the Initial CN value with calibrated parameters input for land use condition from 2006 to 2026: (a) 2006, (b) 2011, (c) 2016, (d) 2021, and (e) 2026

4. Conclusions

Assessing the spatial-temporal changes of land use, particularly in watersheds, is imperative in view of the potential for altering hydrological processes. Mixed agriculture dominates the Sg. Segamat watershed, accounting for more than 75% of the land area, while water bodies occupy less than 2%. Changes in land use capabilities significantly impact flood peak height and flood volumes, showing increases across different return periods under varying land use conditions, both pre- and post-calibration. Moreover, the expansion of built-up areas significantly increased the impermeable surfaces, resulting in higher runoff, as shown in sub-basins 4, 9, and 12, which recorded the highest flood volumes. In the meantime, the conversion of forest land to mixed agriculture resulted in the highest flood peak heights in sub-basins 1, 3, and 11 across all land use conditions in the Sg. Segamat Watershed.

Land use changes seem to be associated with the increased flood peak heights and flood volumes. The comprehension of land use change is necessary because it is useful information to government agencies, policymakers, and local communities for effective flood risk management. Furthermore, predicted outcomes ought to be considered in order to mitigate the effects of land use changes on the watershed's hydrology, eliminating uncertainty and unpredictable events. In light of these findings, government agencies and land use planners must take immediate action to strengthen flood mitigation efforts. This includes constructing efficient drainage systems, especially in areas with impervious surfaces, to ensure that rainwater is properly channelled before reaching the rivers. Additionally, the development and use of flood hazard maps are crucial for identifying high-risk flood zones. It is also essential to enforce regulations that require development projects to incorporate flood mitigation strategies, such as green infrastructure and natural flood retention areas.

The application of the HEC-HMS Model is effective for assessing land use changes and hydrological responses, providing valuable insights for managing water resources and mitigating floods. Nonetheless, the study would be more meaningful if future research

included the development of flood hazard maps, as these can identify flood-prone areas and support communities in assessing their vulnerability. Additionally, incorporating higher-resolution data and supplementary climate variables such as temperature and solar radiation alongside rainfall would enhance the study's accuracy. Although the study has employed Standard Error (SE) to examine model uncertainties, the approach is expanded to include a range of data and methods to examine model uncertainties. Understanding these uncertainties is essential for evaluating the model's overall reliability and validity. Lastly, a multidisciplinary approach, spanning hydrology, engineering, environmental science, and economics, is vital to comprehensively address flood risks.

5. Acknowledgements

The authors gratefully acknowledge the United States Geological Survey (USGS), the Department of Irrigation and Drainage (DID), the Malaysian Department of Agriculture (DOA), and the Department of Survey and Mapping Malaysia (JUPEM) for providing the data in this study. Authors are additionally grateful to Universiti Putra Malaysia−for funding the GP-IPS/2017/9533100 grant, and to Malaysia's Ministry of Higher Education for awarding a PhD scholarship under the MyPhD 15 scheme for this research.

6. References

[1] Makwana N. Disaster and its impact on mental health: a narrative review. J Family Med Prim Care. 2019;8(10):3090-5.
[2] Swain KC, Singha C, Nayak L. Flood susceptibility mapping through the GIS-AHP technique using the cloud. ISPRS Int J Geo-Inf. 2020;9(12):720.
[3] Glago FJ. Flood disaster hazards; causes, impacts and management: a state-of-the-art review. In: Farsangi EN, editor. London: Intech Open; 2021: p. 1-19.
[4] Centre for Research on the Epidemiology of Disasters (CRED). Disaster year in review 2020: Global trends and perspectives. Cred Crunch, 62. [Internet]. 2021 [cited 2023 Apr 7]. Available from: https://reliefweb.int/report/world/cred-crunch-newsletter-issue-no-62-may-2021-disaster-year-review-2020-global-trends-and.
[5] Centre for Research on the Epidemiology of Disasters (CRED). The human cost of disasters - an overview of the last 20 years 2000-2019 [Internet]. 2020 [cited 2023 Apr 7]. Available from: https://reliefweb.int/report/world/human-cost-disasters-overview-last-20-years-2000-2019.
[6] Nguyen HD, Fox D, Dang DK, Pham LT, Viet Du QV, Nguyen THT, et al. Predicting future urban flood risk using land change and hydraulic modeling in a river watershed in the central province of Vietnam. Remote Sens. 2021;13(2):262.
[7] Tabari H. Climate change impact on flood and extreme precipitation increases with water availability. Sci Rep. 2020;10:13768.
[8] Tan ML, Gassman PW, Yang X, Haywood J. A review of SWAT applications, performance and future needs for simulation of hydro-climatic extremes. Adv Water Resour. 2020;143:103662.
[9] Camara M, Jamil NRB, Abdullah AFB, Hashim RB. Integrating cellular automata Markov model to simulate future land use change of a tropical basin. Glob J Environ Sci Manag. 2020;6(3):403-14.
[10] Safiah Yusmah MY, Bracken LJ, Sahdan Z, Norhaslina H, Melasutra MD, Ghaffarianhoseini A, et al. Understanding urban flood vulnerability and resilience: a case study of Kuantan, Pahang, Malaysia. Nat Hazards. 2020;101(2):551-71.
[11] Al-Hussein AAM, Khan S, Ncibi K, Hamdi N, Hamed Y. Flood analysis using HEC-RAS and HEC-HMS: a case study of Khazir River (Middle East—Northern Iraq). Water. 2022;14(22):3779.
[12] D'Ayala D, Wang K, Yan Y, Smith H, Massam A, Filipova V, et al. Flood vulnerability and risk assessment of urban traditional buildings in a heritage district of Kuala Lumpur, Malaysia. Nat Hazards Earth Syst Sci. 2020;20(8):2221-41.
[13] Zawiah WZW, Jemain AA, Ibrahim K, Suhaila J, Sayang MD. A comparative study of extreme rainfall in Peninsular Malaysia: with reference to partial duration and annual extreme series. Sains Malaysiana. 2009;38(5):751-60.
[14] Rosmadi HS, Ahmed MF, Mokhtar MB, Lim CK. Reviewing challenges of flood risk management in Malaysia. Water. 2023; 15(13):2390.
[15] Mohamad S, Ash'aari ZH, Ramli MF, Abdullah R, Rehan BM. Application of a hybrid Cellular Automaton-Markov Model in land use change detection and prediction in flood-prone area, Johor, Malaysia. Planning Malaysia. 2023;21(6):170-84.
[16] Garg V, Nikam BR, Thakur PK, Aggarwal SP, Gupta PK, Srivastav SK. Human-induced land use land cover change and its impact on hydrology. HydroResearch. 2019;1:48-56.
[17] Thoufil Ali MS, Chandran D. Impact of land use land cover change on runoff in Kuttiyadi River Basin. Int J Eng ResTechnol. 2022;11(7):390-403.
[18] Newman G, Kim Y, Joshi K, Liu J. Integrating prediction and performance models into scenario-based resilient community design. J Digit Landsc Archit. 2020;5:510-20.
[19] Ajjur SB, Al-Ghamdi SG. Exploring urban growth–climate change–flood risk nexus in fast growing cities. Sci Rep. 2022;12(1): 12265.
[20] Xin Z, Shi K, Wu C, Wang L, Ye L. Applicability of hydrological models for flash flood simulation in small catchments of hilly area in China. Open Geosci. 2019;11(1):1168-81.
[21] Sharu EH. Development of HEC-HMS model for flow simulation at Dungun River Basin Malaysia. Adv Agric Food Res J. 2021;2(1):a0000169.
[22] El Yousfi Y, Himi M, El Ouarghi H, Aqnouy M, Benyoussef S, Gueddari H, et al. GIS preprocessing for rainfall-runoff modeling using HEC-HMS in Nekkor watershed (Al-Hoceima, Northern Morocco). E3S Web Conf. 2023;364:01005.
[23] Al-Samawi I, Noman A, Khanbari K, Quriaa H, Al-Areeq N, Aklan M. The impacts of land-use change on the runoff characteristics using HEC-HMS model: a case study in Wadi Al-Mulaikhy Sub-Watershed in Sana'a Basin, Yemen. In: Al-Maktoumi A, Abdalla O, Kacimov A, Zekri S, Chen M, Al-Hosni T, et al., editors. Water Resources in Arid Lands: Management and Sustainability. Cham: Springer; 2021. p. 121-30.
[24] Setiawan O, Nandini R. Integration of LULC change/prediction and hydrological modeler for assessment of the effect of LULC change on peak discharge in Sari Watershed, Sumbawa Island, Indonesia. IOP Conf Ser: Earth Environ Sci. 2022;1109:012070.
[25] Ata FM, Toriman ME, Mat Desa S, San LY, Kamarudin MKA. Development of hydrological modelling using HEC-HMS and HEC-RAS for flood hazard mapping at Junjung river catchment. Planning Malaysia. 2023;21(6):116-29.
[26] Mewded M, Abebe A, Tilahun S, Agide Z. Impact of land use and land cover change on the magnitude of surface runoff in the endorheic Hayk Lake basin, Ethiopia. SN Appl Sci. 2021;3(8):742.

[27] Nordin NAS, Hassan Z, Noor NM, Kamarudzaman AN, Ahmadni ASA. Assessing the influence of land use and land cover (LULC) changes on hydrological response of the Timah-Tasoh Reservoir. IOP Conf Ser: Earth Environ Sci. 2024;1303:012030.
[28] Farid M, Pratama MI, Kuntoro AA, Adityawan MB, Rohmat FIW, Moe IR. Flood prediction due to land cover change in the Ciliwung River Basin. Int J Technol. 2022;13(2):356-66.
[29] Liew YS, Mat Desa S, Md. Noh MN, Tan ML, Zakaria NA, Chang CK. Assessing the effectiveness of mitigation strategies for flood risk reduction in the Segamat River Basin, Malaysia. Sustainability. 2021;13(6):3286.
[30] Tan ML, Liang J, Hawcroft M, Haywood JM, Zhang F, Rainis R, et al. Resolution dependence of regional hydro-climatic projection: a case-study for the Johor River Basin, Malaysia. Water. 2021;13(22):3158.
[31] Soo EZX, Jaafar WZW, Lai SH, Islam T, Srivastava P. Evaluation of satellite precipitation products for extreme flood events: case study in Peninsular Malaysia. J Water Clim Change. 2019;10(4):871-92.
[32] Talib SAA, Idris WMR, Neng LJ, Lihan T, Rasid MZA. Irregularity and time series trend analysis of rainfall in Johor, Malaysia. Heliyon. 2024;10(9):e30324.
[33] Eryani GAP, Amerta IMS, Jayantari MW. Model calibration parameter using optimization trial in HEC-HMS for Unda Watershed. IOP Conf Ser: Earth Environ Sci. 2021;930:012040.
[34] Skhakhfa ID, Ouerdachi L. Hydrological modelling of wadi Ressoul watershed, Algeria, by HEC-HMS model. J Water Land Dev. 2016;31(1):139-47.
[35] Carlos Mendoza JA, Chavez Alcazar TA, Zuñiga Medina SA. Calibration and uncertainty analysis for modelling runoff in the Tambo River Basin, Peru, using sequential uncertainty fitting ver-2 (SUFI-2) algorithm. Air Soil Water Res. 2021;14:1-13.
[36] Perodes J, Fornis R. Determination of the initial abstraction ratio and curve number of the upper catchment area of the Sawaga river watershed, Bukidnon [Internet]. Research Square [Preprint]. 2023 [cited 2023 Feb 11]. Available from: https://www.researchsquare.com/article/rs-2852410/v1.
[37] Baig MF, Mustafa MRU, Baig I, Takaijudin HB, Zeshan MT. Assessment of land use land cover changes and future predictions using CA-ANN simulation for Selangor, Malaysia. Water. 2022;14(3):402.
[38] PLANMalaysia. Segamat local plan 2030 draft report (RTD Segamat 2030 (penggantian) untuk cetakan) [Internet]. Malaysia: Department of Town and Country Planning; 2023 [cited 2023 Feb 11]. Available from: http://mpsegamat.gov.my/ms/mds/sumber/penerbitan/rtd-segamat-2030-penggantian-untuk-cetakan. (In Melayu)
[39] Yao Z, Wang B, Huang J, Zhang Y, Yang J, Deng R, et al. Analysis of land use changes and driving forces in the Yanhe River Basin from 1980 to 2015. J Sens. 2021;2021:1-11.
[40] Shikur ZH. Agricultural policies, agricultural production and rural households' welfare in Ethiopia. J Econ Struct. 2020;9:50.
[41] Cotugno A, Smith V, Baker T, Srinivasan R. A framework for calculating peak discharge and flood inundation in ungauged urban watersheds using remotely sensed precipitation data: a case study in Freetown, Sierra Leone. Remote Sens. 2021;13(19):3806.
[42] Romali NS, Yusop Z. Frequency analysis of annual maximum flood for Segamat river. MATEC Web Conf. 2017;103:04003.
[43] Fu S, Yang Y, Liu B, Liu H, Liu J, Liu L, et al. Peak flow rate response to vegetation and terraces under extreme rainstorms. Agric Ecosyst Environ. 2020;288:106714.
[44] Yulianto F, Suwarsono, Nugroho UC, Nugroho NP, Sunarmodo W, Khomarudin MR. Spatial-temporal dynamics land use/land cover change and flood hazard mapping in the Upstream Citarum watershed, West Java, Indonesia. Quaestiones Geographicae. 2020;39(1):125-46.
[45] Abdulkareem JH, Sulaiman WNA, Pradhan B, Jamil NR. Relationship between design floods and land use land cover (LULC) changes in a tropical complex catchment. Arab J Geosci. 2018;11:376.
[46] Santillan JR, Amora AM, Makinano-Santillan M, Gingo AL, Marqueso JT. Analyzing the impacts of land cover change to the hydrologic and hydraulic behaviours of the philippines'third largest river basin. ISPRS Ann Photogramm Remote Sens Spatial Inf Sci. 2019;4:41-8.
[47] Kuntiyawichai K, Sri-Amporn W, Wongsasri S, Chindaprasirt P. Anticipating of potential climate and land use change impacts on floods: a case study of the lower Nam Phong River Basin. Water. 2020;12(4):1158.